NUCL SCI TECH (2016) 27:146
DOI 10.1007/s41365-016-0144-0

An S-band solid-state radio frequency power amplifier used at Shanghai soft X-ray FEL facility

Hong-Li Ding[1,2] · Ming-Hua Zhao[1] · Cheng-Cheng Xiao[1] · Shao-Peng Zhong[1] · Jun-Qiang Zhang[1]

Received: 4 February 2016 / Revised: 25 March 2016 / Accepted: 29 March 2016 / Published online: 31 October 2016

Abstract In this paper, we present the general design methods and parameter measurements of a 1-kW solid-state radio frequency (RF) power amplifier at 2856 MHz, for the soft X-ray free electron laser facility. Three-stage amplification with a 4-way combination is used. An RF switch module is integrated with the solid-state RF power amplifier to convert the continuous wave (CW) signal into pulse signal, with adjustable pulse width. The power gain is measured at 57.7 dB at 60 dBm output. The RF phase noise, which is measured by the low-level RF system, is <0.015 degree (RMS), while the pulse frontier jitter is <5 ns.

Keywords S-band · Solid-state power amplifier · Phase stability

1 Introduction

Free electron laser (FEL), a new form of light source, is generated by using a high-quality relativistic electron beam as the lasing medium. With periodic variation in the magnetic field of the undulator, electromagnetic radiations are amplified by stimulated emission, producing a very bright beam of light [1, 2]. To achieve high brightness of FEL, it is important to stabilize the magnitude and phase of RF power source, with short pulses and good coherency [3].

With the development of RF semiconductor technology such as laterally diffused metal oxide semiconductor (LDMOS), in the recent years, solid-state RF power amplifiers (SSRFPAs) for accelerators have been increasingly used as the leading end of klystron amplifiers [4–6]. Over vacuum tubes, SSRFPAs are advantageous in their availability, reliability, graceful degradation and ease of maintenance [7–9]. Also, an SSRFPA operates at a lower voltage, at which X-rays will not be generated [10]. A number of FEL laboratories have designed kilowatt S-band SSRFPAs [11, 12]. An SSRFPA with a peak power of 1 kW is used to drive the linac klystron of Beijing Electron Positron Collider, China. It uses a three-step amplification process, followed by a 4-way combination to amplify a 10 dB input signal into a 60 dB output signal [13]. The High Power Microwave Engineering Laboratory at Kwangwoon University, South Korea, uses a 1.5-kW SSRFPA as a radar transmitter. The power amplifier operates at 2.7–2.9 GHz with eight stages of amplification, and the peak output power at 1.61 kW [14]. To drive a 2-MW klystron of a linac, the Information and Communication Technology Institute at Isfahan University of Technology, Iran, developed a 2-kW multi-stage S-band SSRFPA, with 16 amplifier modules of 180 W each, producing a peak power of 2 kW and adjustable pulse width of 2–10 μs [15].

A compact soft X-ray free electron laser test facility is now underway at Shanghai Institute of Applied Physics (SINAP), Chinese Academy of Science [16, 17]. Figure 1 shows schematically an RF station of SXFEL. The reference RF signal is modulated by a vector modulator in the MTCA4.0 LLRF system, amplified by a solid-state

✉ Ming-Hua Zhao
zhaomh@sinap.ac.cn

1 Shanghai Institute of Applied Physics, Chinese Academy of Sciences, Zhangjiang, Shanghai 201800, China

2 University of Chinese Academy of Sciences, Beijing 100049, China

Fig. 1 RF system layout of SXFEL

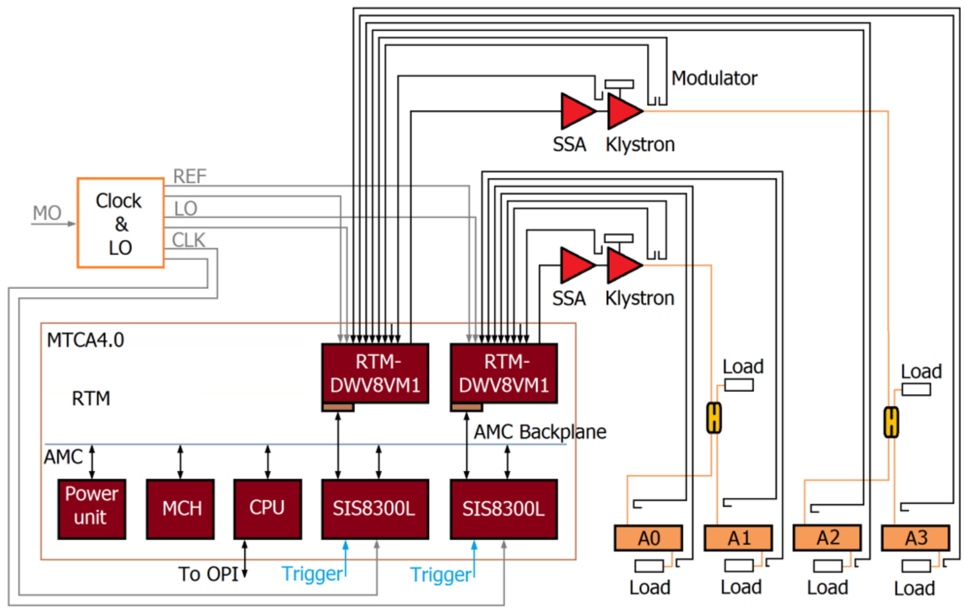

amplifier and a klystron and finally fed into the two S-band accelerating structures. The SXFEL device requests highly in the RF signal's phase stability [18–20]. At S-band, the total phase noise should be <0.09°. The phase noise can be divided into the individual components by assuming that the jitter contribution is uncorrelated and equally distributed among the subsystems.

$$\delta_{\varphi} = \sqrt{(\delta_{\varphi})^2_{\mathrm{MO}} + (\delta_{\varphi})^2_{\mathrm{CLK\&LO}} + (\delta_{\varphi})^2_{\mathrm{LLRF}} + (\delta_{\varphi})^2_{\mathrm{AMP}} + (\delta_{\varphi})^2_{\mathrm{KLY}}}, \tag{1}$$

where δ_{φ} is the total phase noise; and the subscriptions of MO, CLK&LO, LLRF, AMP and KLY denote master oscillator, clock and local oscillator, low-level RF system, solid-state power amplifier and klystron, respectively. The phase noise requirements for the RF system in the SXFEL device are listed in Table 1. The phase noise distributed to the solid-state power amplifier should be <0.015°. According to the requirements above, we developed a three-stage SSRFPA working at 2856 MHz with an output power of 1 kW. This amplifier can be used to drive the klystron of SXFEL accelerator.

In this paper, we report the SSRFPA structure, functions of each module and the experiment results.

Table 1 The 2856 MHz phase noise requirements of RF equipment

Parameter	Value (RMS)
Phase noise requirement	87.5 fs/0.09°
Master oscillator	40 fs/0.041°
Clock &LO	40 fs/0.041°
Low-level RF system	20 fs/0.021°
Solid-state amplifier	15 fs/0.015°
Klystron	61 fs/0.063°

2 Description of the SSRFPA

2.1 General description

The 1-kW SSRFPA consists of a RF switch module, a pulse control module, a pre-amplifier module, a mid-amplifier module, a 4-way power divider, 4 final amplifier modules and a 4-way power combiner, as shown schematically in Fig. 2. The RF switch is used to convert the input CW signal into a pulse signal. The pulse control module is used to adjust the pulse width. An RF signal passes through the pre-amplifier and mid-amplifier and is

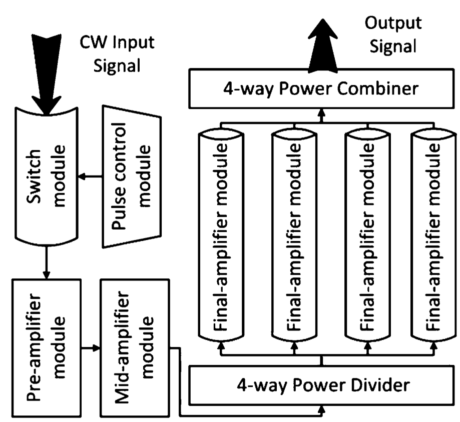

Fig. 2 Schematics of the 1-kW power amplifier

then split into four paths by the power splitter to drive the final amplifier individually. Lastly, it goes through the power combiner as an output. The entire amplifier is able to amplify a 0 dBm input signal into a 59.55 dBm output signal, with an amplification gain of 59 dB.

2.2 The final amplifier module

The final amplifier module is the core component of the SSRFPA. As shown in Fig. 3a, the transistor is MRF8P29300RH from Freescale Semiconductor Inc., TX, USA, for its high output power and good stability. It has two subtransistors, working in the AB class mode [21].

The design of matching network has been optimized using the Advanced Design system (ADS) software and adjusted according to the actual results. Due to the transistor's push–pull amplifier design, it is essential to include an unbalanced-to-balanced signal converter structure aka balun in the matching network. Micro-strip lines T1–T4 and T13–T16 thus act as baluns. The two isolators ISO1 and ISO2 are at the input and the output of the power amplifier, respectively, to isolate the reflected current at the input and output, thus protecting the transistor [22]. The actual module is shown in Fig. 3b.

The mid-amplifier module is identical to the final amplifier module in structure and performance.

2.3 Other modules

The output pulse of the RF switch module has an outstanding leading and trailing edges.

The pulse control module is used to render the input time-to-live (TTL) signal adjustable. At the input end, an anti-electromagnetic interference device is used to increase the signal's stability.

A schematic diagram of the pre-amplifier module is shown in Fig. 4. It consists of four cascaded power transistors, with three isolators in the middle protecting the circuit. An adjustable attenuator is added at the circuit input to adjust the amplification gain. At the DC input, a DC power protection network protects the transistor from breakdown. The power combiner and divider is made of three 90° electrical bridges, each of which uses a 1/4 wavelength micro-strip line to delay the signal phase by 90°.

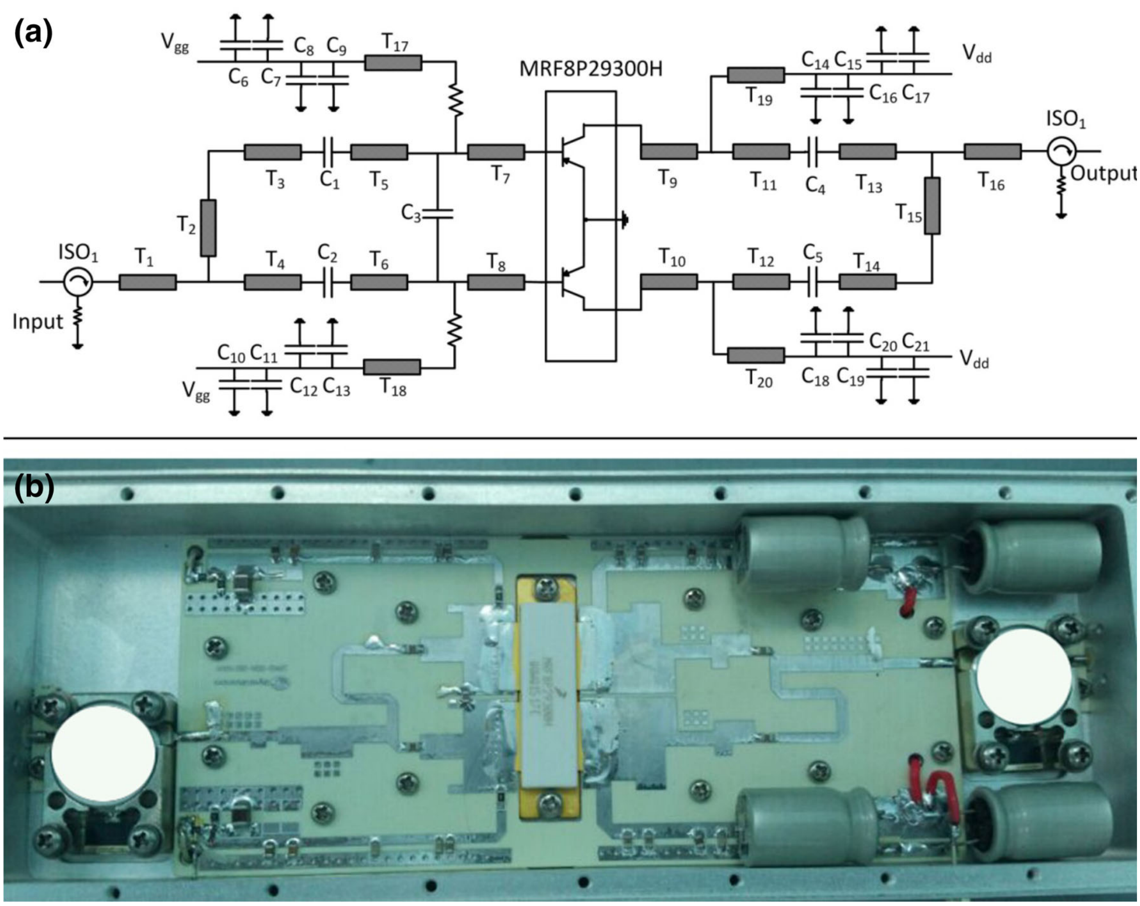

Fig. 3 Schematics (**a**) and photograph (**b**) of the amplifier module

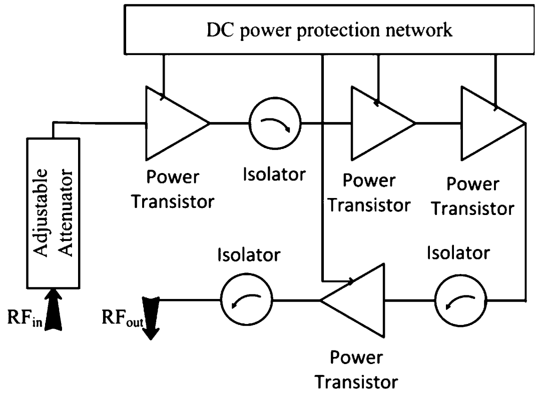

Fig. 4 Schematic diagram of the pre-amplifier module

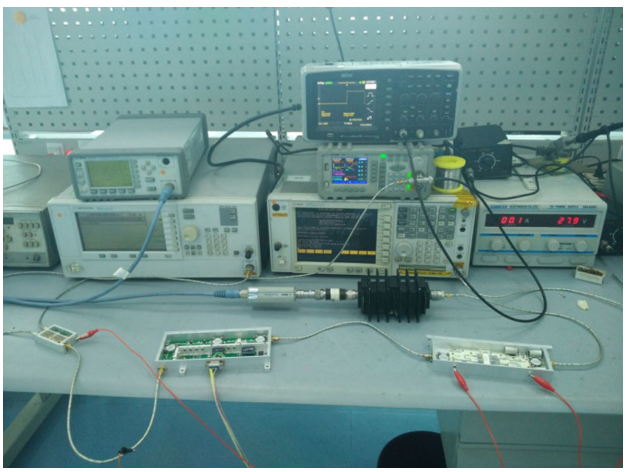

Fig. 5 Parameter measurement platform of the amplifier

3 Results and discussion

3.1 The module performance tests

A parameter measurement platform (Fig. 5) was established, with a signal generator, a DC supply, a waveform generator, a power meter, a spectrum analyzer (SPA), a vector network analyzer (VNA) and a power attenuator. The test devices included a pulse switch module, a pre-amplifier module and a mid-amplifier module.

The signal generator (E8247C, frequency range: 250 kHz–20 GHz, power level: 15 dBm), the power meter (E4416A), the spectrum analyzer (E4440A, 3 Hz–26.5 GHz) and the VNA (E5071B, 300 kHz–8.5 GHz) are manufactured by Agilent Technologies, CA, USA. The waveform generator, TATFA20B, is from Atten Instruments.

The 4-port VNA is used to measure the S parameter, gain and phase characteristics of the test module. Its power and frequency scanning options are adjusted to suit the test module's capability. The power meter is used to measure the amplifier module's output power. The SPA is used to measure the phase noise. An input signal, from in a signal source, passes through the module under test. It is attenuated by a 40 dB attenuator and transmitted to the power meter and SPA. The signal generator generates a pulse signal of fixed width to provide the pulse control module with the original waveform.

Figure 6 shows the change in spectrum curve after signal amplification. A phase noise degradation of 0.57 dB can be seen in the single sideband of 50 kHz. The pulse transition response rate is higher than other digital circuit

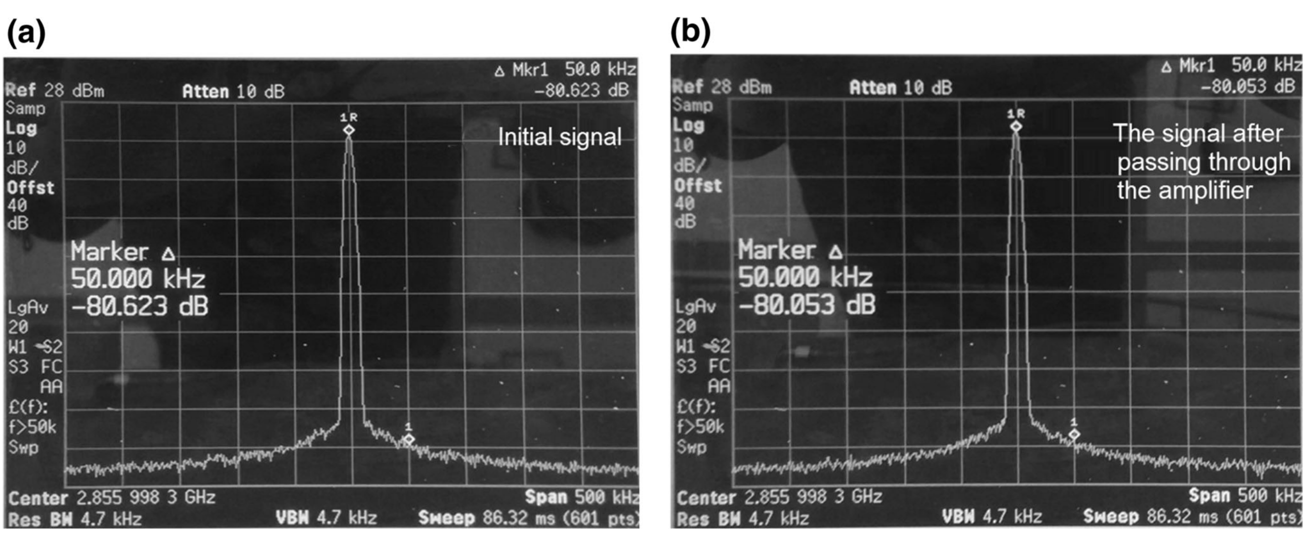

Fig. 6 The change of the spectrum curve

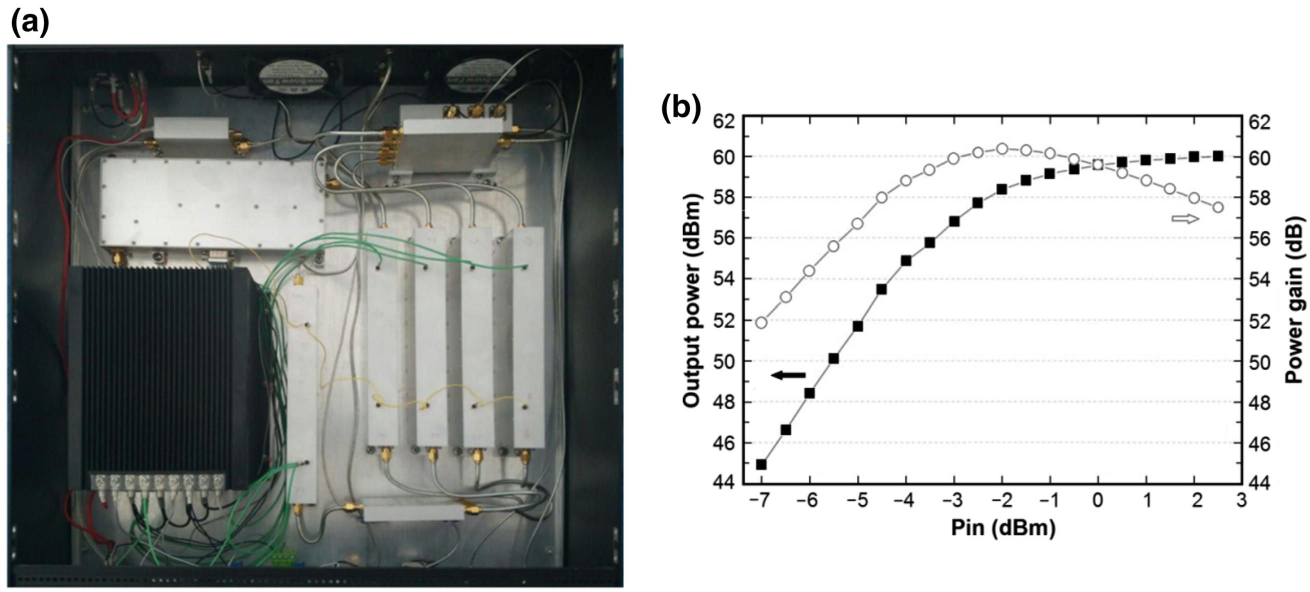

Fig. 7 The S-band solid-state power amplifier (**a**) and its output power and power gain (**b**)

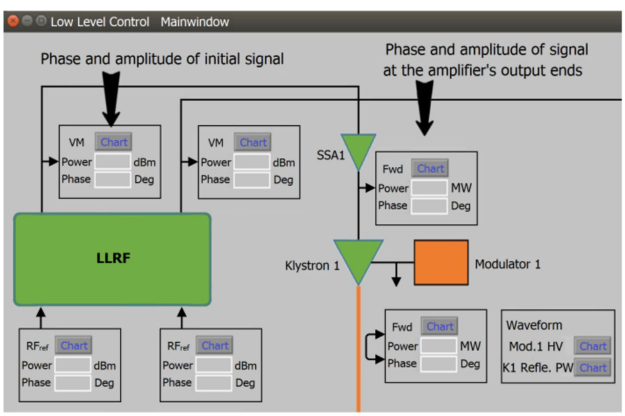

Fig. 8 LLRF measurement system interface

switch of the same cost. Also, the anti-electromagnetic interference device at the pulse switch's input end lowers external interferences effectively.

3.2 Performance of the SSRFPA

The assembled S-band solid-state power amplifier is shown in Fig. 7a. Its input power, output power and power gain are shown in Fig. 7b. It can be seen that the maximum power output was 59.9 dBm, with a power gain of 57.4 dB.

The low-level RF system to measure the phase stability developed at SINAP consists of the CLK & LO, MTCA4.0 (with the down converter DWC8VM1 and digitizer SIS8300L), and solid-state amplifier (see Fig. 1).

The LLRF captures the 2856 MHz signal at the amplifier's input and output ends separately and then converts the frequency to 25.5 MHz. So, its samplings are through a 102 MHz clock. The data flow after sampling is $I.$, $Q.$, $-I.$ and $-Q.$, where $I.$ and $Q.$ represent the in-phase and quadrature, respectively. After demodulating IQ, the I and Q signals can be obtained. The signals are calculated by an FPGA board using a CORDIC algorithm to finally obtain

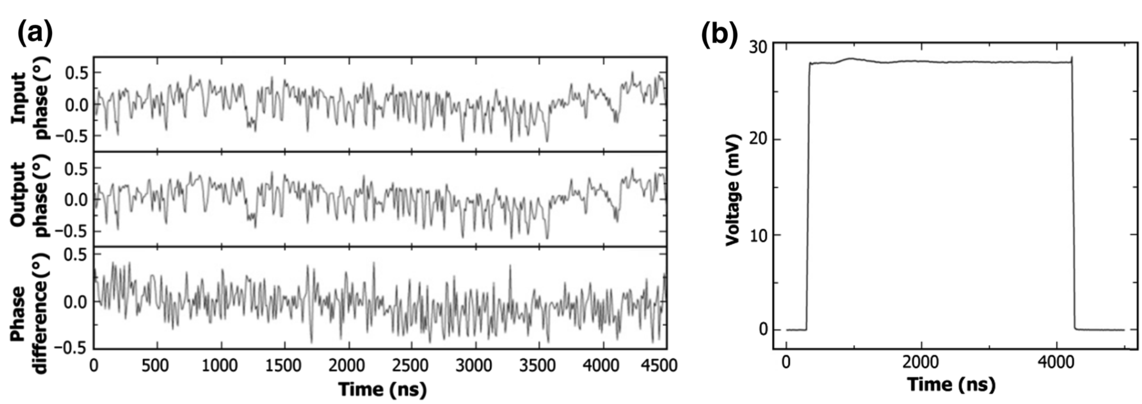

Fig. 9 Measured phase jitter of RF signal (**a**) and Pulse envelope of output signal (**b**)

the phase jitter values at the amplifier's input and output ends. An interface of the LLRF measurement system in Fig. 8 displays the phase and amplitude of signals from the amplifier's input and output ends. The data collected are processed by MATLAB.

Figure 9a shows the phase jitter values at the amplifier's input and output ends and their differences as well. Root-mean-square (RMS) jitter is an important parameter to describe the phase jitter. The time point of the n^{th} zero-crossing leading edge is referred to as t_n The n^{th} period is then defined as $T_n = t_{n+1} - t_n$. The time difference varies with n as a result of noise in the circuit. This causes a deviation of $\Delta T_n = T_n - T_{\text{mean}}$ from the mean period T_{mean}. The quantity ΔT_n is an indication of jitter. RMS jitter can be written as:

$$\Delta T_{\text{RMS}} = \lim_{N \to \infty} \sqrt{\frac{1}{N} \sum_{n=1}^{N} (\Delta T_n)^2}. \tag{2}$$

RMS jitter describes magnitude of the signal fluctuations [23]. Using MATLAB, RMS phase jitter of the extracted samples is at 0.014°, while the system's requirement is < 0.015°. It ensured the stability of the amplitude and phase of FEL's input RF signal and is especially meaningful to the highly bright and stable FEL. In Fig. 9b, a single pulse envelope at output port shows that its frontier jitter is <5 ns. After calculations, the intra-pulse flat top's RMS jitter is 0.16 %.

4 Conclusion

An S-band solid-state RF amplifier has been developed successfully. The measurement results show that the output power is over 1 kW, the intra-pulse flat top is <0.2 % RMS, and the RF phase stability is <0.015°. Low phase noise and commendable flatness in the pulse envelope are extremely meaningful to improve the stability and efficiency of FELs. All these are helpful for FELs to attain table performances.

Acknowledgments The authors are grateful to Zhi-Yin Cheong for language assistance in the preparation of this paper. We also thank Zhe Yin for experimental supports and for his valuable suggestions and guidance.

References

1. P. Schmüser, M. Dohlus, J. Rossbach, Ultraviolet and soft X-ray free-electron lasers: introduction to physical principles, experimental results, technological challenges. Spring. Tracts Mod. Phys. (2009). doi:10.1007/978-3-540-79572-8
2. H.X. Deng, Feasibility study on optical vortex generation at Shanghai deep ultraviolet free-electron laser. Nucl. Sci. Tech. **25**, 010101 (2014). doi:10.13538/j.1001-8042/nst.25.010101
3. Z.T. Zhao, S.Y. Chen, L.H. Yu, et al., Shanghai Soft X-Ray Free Electron Laser test Facilty, in Proceedings of IPAC2011, San Sebastián, Spain, (2011). http://accelconf.web.cern.ch/accelconf/ipac2011/papers/thpc053.pdf
4. C. Chen, Y. Hao, H. Feng et al., An X-band GaN combined solid-state power amplifier. J. Semicond. **30**, 095001 (2009). doi:10.1088/1674-4926/30/9/095001
5. B.V. Ramarao, S. Sonal, J.K. Mishra et al., Development of 3 kW at 325 MHz solid-state RF power amplifier using. Nucl. Instrum. Meth. A **735**, 283–290 (2014). doi:10.1016/j.nima.2013.09.053
6. P. Marchand, T. Ruan, F. Ribeiro et al., High power 352 MHz solid state amplifiers developed at the Synchrotron SOLEIL. Phys. Rev. Special Top-Accel. Beams. **10**, 112001 (2007). doi:10.1103/PhysRevSTAB.10.112001
7. V. G. Hansen, Radar systems trade-offs, vacuum electronics vs. solid-state. IEEE Int Vacuum Electron Conf. pp. 12–13 (2004).doi:10.1109/IVELEC.2004.1316173
8. M. D. Giacomo, Solid-state RF amplifiers for accelerator applications, in Particle accelerator conference, Vancouver, Canada, pp. 757–761. http://epaper.kek.jp/PAC2009/papers/tu4rai01.pdf. 2009
9. R.S. Symons, Modern microwave power sources. IEEE AESS Syst. Mag. **17**, 19–26 (2002). doi:10.1109/62.978360
10. A. Schirmer, Emission of parasitic X-rays from military radar transmitters and exposure of personnel: towards a retrospective assessment, in 2nd European IRPA Cong, radiation protection, Paris. http://www.iaea.org/inis/collection/NCLCollectionStore/_Public/39/016/39016846.pdf. 2006
11. L.J. Zhang, A new generation of S-band solid state 16 kW transmitter for ATC primary radar. IEEE Radar Conference. pp. 191–193, (1999). doi:10.1109/NRC.1999.767311
12. K. Nakade, K. Seino, A. Tsuchiko, Development of 150 W S-band GaN solid state power amplifier for satellite use, in Asia-pacific microwave conference, pp. 127–130 (2010). ISBN: 978-1-4244-7590-2
13. F.L. Zhao, 1 kW S-band RF solid state amplifier for BEPC linac microwave driver system. High Energy Phys. Nucl. Phys. **27**, 1031–1033 (2003). doi:10.3321/j.issn:0254-3052.2003.11.019
14. J. H. Joo, G. W. Choi, S. M. Jang, et al., 1.5 kW solid state pulsed microwave power amplifier for S-band radar application, in Radio and Wireless symposium. 2006 IEEE, pp. 171–174 (2006). doi:10.1109/RWS.2006.1615122
15. S. R. Motahari, H. Pahlevaninezhad, D.S. Beyragh, Design and implementation of a high power s-band solid-state pulsed amplifier for LINAC, in ISSSE, 2010 International Symposium 1, 1–4 (2010). doi:10.1109/ISSSE.2010.5607080
16. C.P. Wang, W.C. Fang, D.C. Tong et al., Design and study of a C-band pulse compressor for the SXFEL linac. Nucl. Sci. Tech. **25**, 020101 (2014). doi:10.13538/j.1001-8042/nst.25.020101
17. J.H. Tan, Q. Gu, W.C. Fang et al., X-band deflecting cavity design for ultra-short bunch length measurement of SXFEL at SINAP. Nucl. Sci. Tech. **25**, 060101 (2014). doi:10.13538/j.1001-8042/nst.25.060101
18. G.L. Wang, J.Q. Zhang, L. Li et al., The control and measurement of high power high-gradient acceleration structures. Nucl. Sci. Tech. **26**, 030102 (2015). doi:10.13538/j.1001-8042/nst.26.030102
19. C. Schmidt, G. Ayvazyan, V. Ayvazyan, et al., Recent development of the European XFEL LLRF system, in Proceedings Of Ipac2013, Shanghai, China. (2013). http://ir.ihep.ac.cn/handle/311005/188024

20. G. Patrick, O. Shea, H.P. Freund, Free-electron lasers: status and applications. Science **292**, 1853–1858 (2001). doi:10.1126/science.1055718
21. http://www.nxp.com/
22. J. M. Godefroy, F. Ribeiro, T. Ruan, et al., MOSFET RF power amplifier for accelerator applications, in 6th European Particle Accelerator Conference. pp. 22–26 (1998). http://epaper.kek.jp/e98/PAPERS/TUP04A.PDF
23. F. Herzel, B. Razavi, A study of oscillator jitter due to supply and substrate noise. Circ. Syst. II Analog. Digit. Signal Process. **46**, 56–62 (1999). doi:10.1109/82.749085